JTTEE5 12:199-207

Influence of Deposition Temperature on Mechanical Properties of Plasma-Sprayed Hydroxyapatite Coating on Titanium Alloy With ZrO_2 Intermediate Layer

Bang-Yen Chou and Edward Chang

(Submitted 2 October 2001; in revised form 1 February 2002)

Hydroxyapatite coatings were plasma sprayed on the Ti6Al4V substrate with and without an intermediate ZrO_2 layer; meanwhile the temperatures of substrates were varied at 90, 140, and 200 °C. The coatings were subjected to the standard adhesion test per ASTM C633-79. The purpose of the investigation was to study the effects of those processing variables on the bonding strength and failure behavior of the system. It is found that the bonding strengths of HA/ZrO_2 and HA coatings generally decrease with increasing substrate temperature, except for the HA/ZrO_2 coating deposited at 200 °C. The rationale of the results is attributed to the residual stress reported in the literature. Introducing ZrO_2 bond coat is found to significantly promote the bonding strength of HA coating. The possible strengthening mechanism is the rougher surface of ZrO_2 bond coat and the higher toughness of ZrO_2, which provide the mechanical strengthening effects. The slightly denser HA in 200 °C deposited HA coating cannot explain the high bonding strength of the HA/ZrO_2 coating, nor the mechanical strengthening effect of ZrO_2 intermediate layer should apply. It is believed that a stronger diffusion bonding is formed at the interface of HA and ZrO_2, which increases the bonding between them chemically. The bonding strengths of HA/ZrO_2 and HA coatings are correlated with the area fraction of adhesive failure of the coatings. The correlation explains the findings in this study.

Keywords bond coat, deposition temperature, hydroxyapatite, mechanical properties, plasma spraying

1. Introduction

Hydroxyapatite [$Ca_{10}(PO_4)_6(OH)_2$, HA] is one of the biomaterials often used in orthopedics and dentistry.[1] When used as a coating material on metallic implants, the assembly combines the merits of strength, ductility and ease of fabrication of the metals with the biocompatibility associated with the HA.[2-5]

Among the methods of fabricating HA coating on metallic implants, plasma-spraying technique appears to be most favorable.[6,7] It has been documented that plasma-sprayed coatings suffer from the low adhesion between coating and substrate, as well as the low cohesion within the coating.[8,9] In evaluating the performance and stability of HA coating in the load-bearing situation after long-term follow-up, researchers suggested the presence of a potentially weak HA/substrate interface (adhesive failure) or within HA per se (cohesive failure), rather than at HA/bone interface.[10-12] It was also argued that the adhesive strength dominated the performance of a plasma-sprayed coating with respect to the failure occurred near the coating/substrate interface.[9]

To improve the bonding at HA/Ti-6Al-4V interface, it has been suggested that an intermediate layer (bond coat) can be introduced between HA and Ti-6Al-4V substrate.[13-15] In a preliminary interface investigation of HA top coat/ZrO_2 bond coat/Ti-6Al-4V substrate coating system,[16] an apparent elemental interdiffusion between HA and ZrO_2 was observed by transmission electron microscopy (TEM) for the preheated ZrO_2-coated Ti-6Al-4V substrate. The average substrate temperature of 200 °C was maintained during the deposition of HA topcoat.[16] Hence, the effect of substrate temperature on the bonding strength of HA/ZrO_2 coating on Ti-6Al-4V substrate is of interest.

Residual stress in plasma-sprayed coatings is an inherent problem influenced by the substrate temperatures during secondary cooling,[17] which is caused by the thermal expansion mismatch between the coating and substrate with a complicated mechanism during solidification of the coating.[18,19] The performance of the coating can be affected by the magnitude of the residual stress.[20] Hence, the aim of this present study was to investigate the effect of substrate temperature on the bonding strength and fracture behavior of HA coating on Ti-6Al-4V substrate (referred to as Ti substrate), and HA coating on Ti-6Al-4V substrate with an intermediate ZrO_2 layer (referred to as ZrO_2/Ti substrate).

2. Materials and Methods

2.1 Powder Preparation

Powders suitable for plasma spraying were prepared as follows. Hydroxyapatite and zirconia powders were received from commercial suppliers (Merck, Frankfurt, Germany and TOSOH, Tokyo, Japan, respectively). Zirconia powder used was cubic ZrO_2 (JCPD 30-1468) stabilized with 8 mol% Y_2O_3

Bang-Yen Chou and **Edward Chang,** Department of Materials Science and Engineering, National Cheng Kung University, Tainan 701, Taiwan. Contact e-mail: edchanghs@yahoo.com.

Table 1 Plasma-Spraying Parameters Employed for Preparation of the Coatings in the Study

Parameters	HA Top Coat	ZrO_2 Bond Coat
Primary gas (Ar), flow rate (1 min^{-1})	41	41
Secondary gas (H_2), flow rate (1 min^{-1})	8	10
Powder carrier gas (Ar), flow rate (1 min^{-1})	3	3
Powder feed rate (g min^{-1})	33	33
Power (kW)	40.2	42
Stand-off distance (cm)	7.5	7.5
Surface speed (cm min^{-1})	8000	8000
Traverse speed (cm min^{-1})	60	60
Initial substrate temperatures	5 °C (C), 25 °C (N), 50 °C (H)	25°C

Plasma spraying was performed with a Plasma-Technik system (M-1100C).

(TZ8Y powder). Typical particle sizes of HA and TZ8Y powders (at 50% cumulative mass percent) were measured as 7.0 and 0.2 μm (Sedigraph 5100, Micromeritics Instrument Corp., Norcross, GA), respectively. Both HA and ZrO_2 powders were agglomerated with 10 wt.% aqueous polyvinyl alcohol (PVA) solution (concentration, 5 wt.%), and sieved to the desired particle size (125~177 μm). Finally, the sieved powders were heated at 600 °C for 1 h to volatilize the PVA binder and sintered at 1000 °C for 4 h to consolidate the particles.

2.2 Specimen Fabrication

As-sintered ZrO_2 powder was first coated onto the Al_2O_3 grit-blasted substrate of standard Ti-6Al-4V alloy (ASTM F-136) to form an intermediate ZrO_2 layer by plasma spraying. The average size of Al_2O_3 grit was 300 μm, and the air pressure of 6 kg/cm^2 was applied during the grit-blasting of the substrates. Then, as-sintered HA powder was applied as topcoat onto the surface of the intermediate ZrO_2 bond coat. To understand the effect of substrate temperature on the characteristics of the HA coating on Ti substrate as well as the HA coating on ZrO_2/Ti substrate, the Ti and ZrO_2/Ti substrates each with three initial temperatures of 5, 25 and 50 °C were prepared. The plasma-spraying parameters used are shown in Table 1. By control of the cooling condition during manufacturing, the substrate temperatures after plasma spraying HA topcoat were measured as 90, 140, and 200 °C, respectively. The corresponding produced coatings are denoted as C-HA, N-HA and H-HA for HA coating on Ti substrate; and C-HA/ZrO_2, N-HA/ZrO_2, and H-HA/ZrO_2 for HA on ZrO_2/Ti substrate, respectively. The thickness of HA coating on Ti substrate was 150 μm. For HA coating on Ti substrate with ZrO_2 intermediate layer, the thickness of ZrO_2 bond coat was 15 μm and the total thickness of HA/ZrO_2 coating was 150 μm.

2.3 Materials Characterization

Disk specimens cut from rods measured 2.54ϕ × 5.5*L* cm were coated with HA coating, ZrO_2 bond coat, or HA/ZrO_2 composite coating on the end surface for materials characterization. The phase identity of ZrO_2 bond coat and HA top coat was examined by x-ray diffractometry (XRD) (Rigaku D/MAX III.V, Tokyo, Japan) using Cu K_α radiation, operated at 30 kV, 20 mA with scan speed of 1° (2θ)/min. Scanning electron microscope (SEM) (Philips XL-40 FEG, Eindhoven, The Netherlands), equipped with energy dispersive x-ray spectrometer (EDS), was used for the observation of morphologies of the grit-blasted Ti substrate, ZrO_2 bond coat and HA top coat as well as for the examination of cross-sectional microstructure and chemical analysis. The surface roughness of grit-blasted Ti substrate, ZrO_2 bond coat, and HA topcoat was measured by a surface roughness tester (Surfcorder SE-40D, Kosaka Laboratory Ltd, Tokyo, Japan).

It could be argued that the phase composition of the HA coatings near the HA/substrate interface, compared with the top layer of HA coatings, should be more relevant to the bonding strength measurements. To clarify this point, the HA/ZrO_2 coatings were thinned till 30-50 μm left on the substrate, and the specimens were also subjected to x-ray diffraction analyses to determine the contents of impurity phases in C-, N-, and H-HA/ZrO_2 coatings.

2.4 Bonding Strength and Fractography

Cylindrical Ti-6Al-4V alloy rods, mentioned in section 2.3, were used as substrates for bonding strength measurements. Bonding strength was measured using an adhesion test (ASTM C633-79) designed for plasma-sprayed coatings. Each test specimen was comprised of a substrate rod, to which the HA/ZrO_2 and HA coatings were applied, and a loading rod. The nominal thickness of the coatings was 150 μm. Before deposition of coatings, the substrate rods were degreased to remove organic contaminants and blasted with Al_2O_3 grit to effect surface roughness. The facing of the loading rods were also grit-blasted and attached to the surfaces of HA coatings using a special adhesive glue (METCO EP-15). The segments were held perpendicularly and the glue was cured in an oven at 180 °C for 2h. The couples were then subjected to tensile tests at a constant crosshead speed of 0.02 mm/s until failure. For each testing material, ten specimens were used, and the bonding strength data were reported as the mean ±S.D. To characterize the fractographs, the optical pictures of the fracture surfaces from bonding strength specimens were scanned as image files in a computer and analyzed by the OPTIMAS 6.0 software. The significant differences between the measured data were determined by statistical *t*-test (one-tailed test, $p < 0.005$).

3. Results

3.1 Coating Characterization

Figure 1 shows the XRD spectra of as-sintered ZrO_2 powder (Fig. 1a) and as-sprayed ZrO_2 bond coat on the Ti substrate (Fig. 1b). The original source of ZrO_2 powder stabilized with 8 mol% Y_2O_3 (TOSOH) is a cubic phase (JCPD 30-1468). Comparing Fig. 1 with the standard JCPD 30-1468 reveals that no phase change occurs after sintering (Fig. 1a) and plasma spraying (Fig. 1b). The appearance of Ti (101) and Ti (002) peaks (JCPD 44-1294) in the XRD spectrum of Fig. 1(b) is caused by the penetrating x-ray beam through the thin layer of ZrO_2 to reach the Ti substrate. Figure 2 shows the XRD spectra of as-sintered HA powder (Fig. 2a) and as-sprayed HA topcoat deposited on the bond coat (Fig. 2b). From Fig. 2(a), it is obvious that a well-crystallized HA powder after sintering suitable for plasma

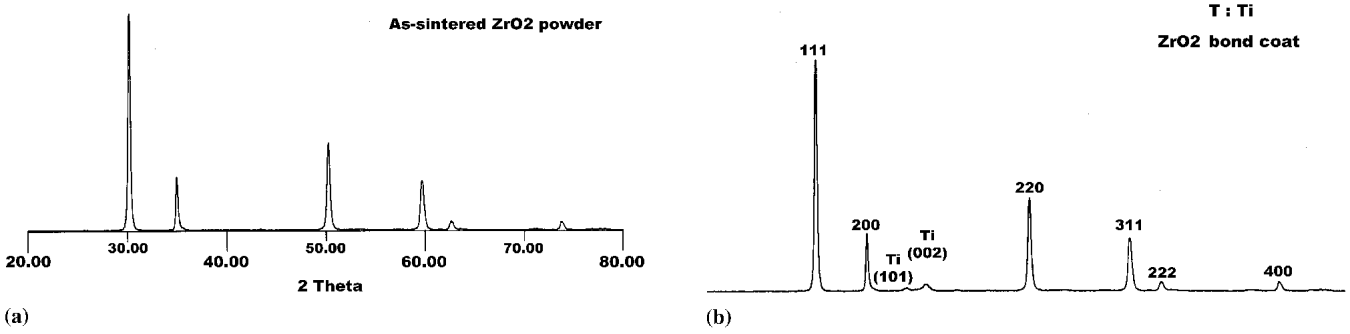

Fig. 1 XRD pattern of **(a)** as-sintered ZrO_2 powder and **(b)** as-sprayed ZrO_2 bond coat of the HA/ZrO_2 coating

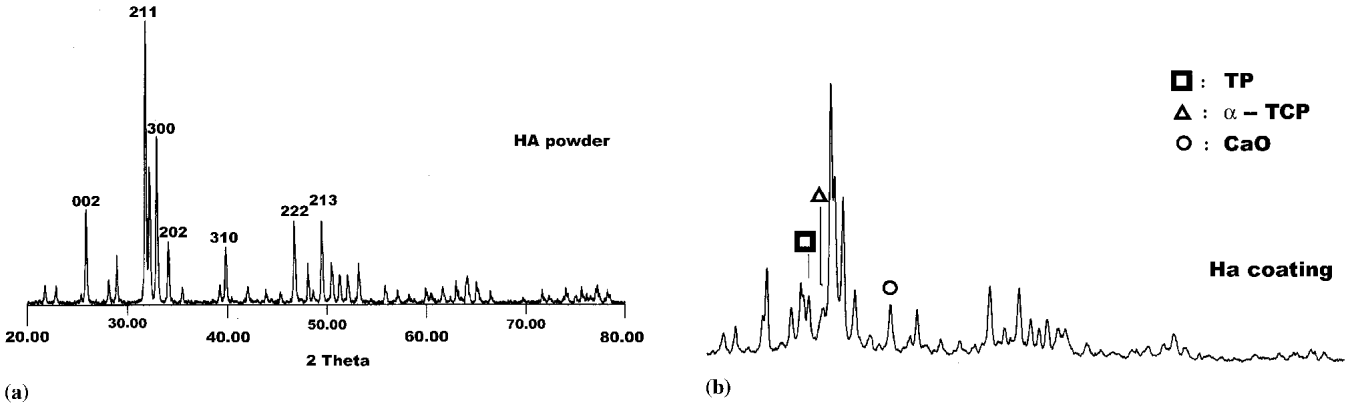

Fig. 2 XRD pattern of **(a)** as-sintered HA powder and **(b)** as-sprayed HA top coat of a typical HA/ZrO_2 coating

spraying was obtained. However, impurity phases of α-tricalcium phosphate (α-TCP), tetracalcium phosphate (T.P.) and CaO are present in the HA top coat as shown in Fig. 2(b). Moreover, Table 2 shows the contents of impurity phases in HA coatings near the HA/ZrO_2 interface, for C-, N-, and H-HA/ZrO_2 specimens prepared under 90, 140, and 200 °C substrate temperatures, respectively.

The results of surface roughness measurements of the grit-blasted Ti substrate, ZrO_2 bond coat, and HA top coat deposited with different substrate temperatures (C-, N-, and H-HA/ZrO_2) are summarized in Table 3, where the results of HA coatings (C-, N-, and H-HA) are also listed. The surface roughness of ZrO_2 bond coat is 5.7 ± 0.2 μm (Ra, mean ± S.D.), while that of grit-blasted Ti substrate is 3.6 ± 0.1 μm. The ZrO_2 bond coat provides a rougher surface than the grit-blasted Ti-6Al-4V for the deposition of HA in the HA/ZrO_2 coating. Consequently, the surface roughness of C-HA/ZrO_2, N-HA/ZrO_2, and H-HA/ZrO_2 coatings are higher than C-HA, N-HA, and H-HA coatings, respectively. As shown in Table 3, the surface roughness of H-HA/ZrO_2 is slightly lower than that of C-HA/ZrO_2 and N-HA/ZrO_2. The similar phenomenon is also seen in the H-HA compared with C-HA and N-HA.

The SEM surface morphologies of the grit-blasted Ti substrate and the as-sprayed ZrO_2 bond coat are shown in Fig. 3. It is seen that the surface of ZrO_2 bond coat is rougher than that of grit-blasted Ti-6Al-4V substrate. The SEM surface morphologies of the as-sprayed HA top coat deposited on ZrO_2/Ti substrate with different substrate temperatures are shown in Fig. 4.

Table 2 The Contents of Impurity Phases in HA Coatings, in wt.%, Near the HA/ZrO_2 Interface for Specimens Prepared Under Different Substrate Temperatures

Impurity Phases	90 °C	140 °C	200 °C
α-TCP	3.9	3.1	1.5
TP	1.4	2.1	2.0
CaO	2.7	3.3	2.5

Table 3 Results of Surface Roughness Measurements (Ra)

Substrate/Coatings	HA/ZrO_2 Coating	HA Coating
Grit-blasted Ti substrate	3.6 ± 0.1	3.6 ± 0.1
ZrO_2 bond coat	5.7 ± 0.2	…
C-series HA coating	10.4 ± 0.3	9.8 ± 0.5
N-series HA coating	10.2 ± 0.4	9.4 ± 0.4
H-series HA coating	9.7 ± 0.2	8.3 ± 0.3

Values are given as mean ± S.D. from 10 test data.

This figure shows that the surface of H-HA/ZrO_2 coating is flatter than that of C-HA/ZrO_2 and N-HA/ZrO_2 coatings, however no distinct differences in surface morphology can be seen between C-HA/ZrO_2 and N-HA/ZrO_2. Hence, Fig. 3 and 4 substantiate the results of surface roughness measurements in Table 3. The SEM cross-sectional view of a typical HA/ZrO_2 coating on Ti substrate is shown in Fig. 5, where EDS line scan indicates the Ca element distribution.

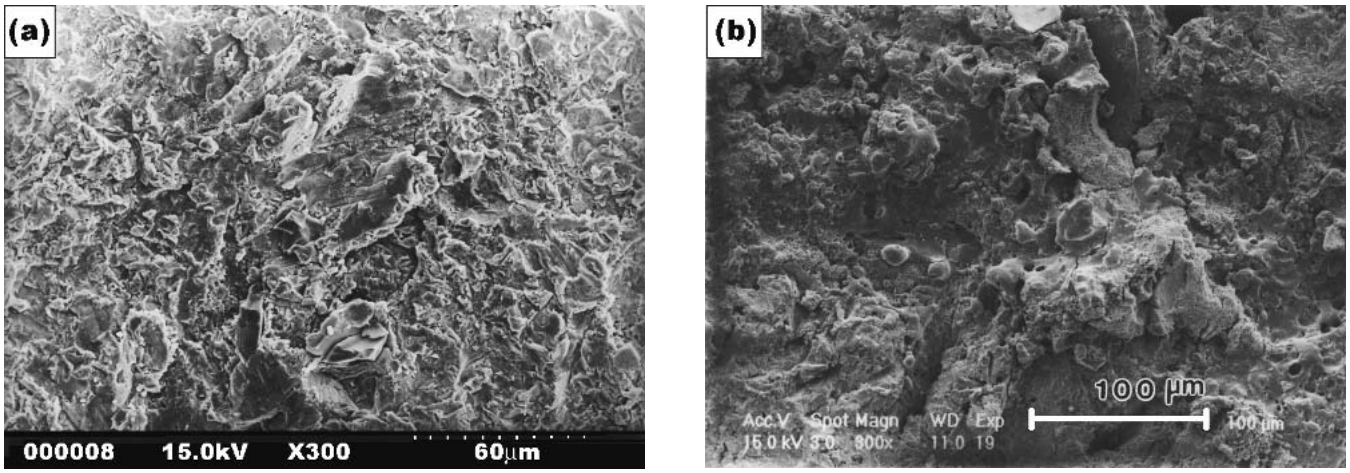

Fig. 3 SEM surface morphologies of **(a)** Al_2O_3 grit-blasted Ti-6Al-4V substrate and **(b)** as-sprayed ZrO_2 bond coat

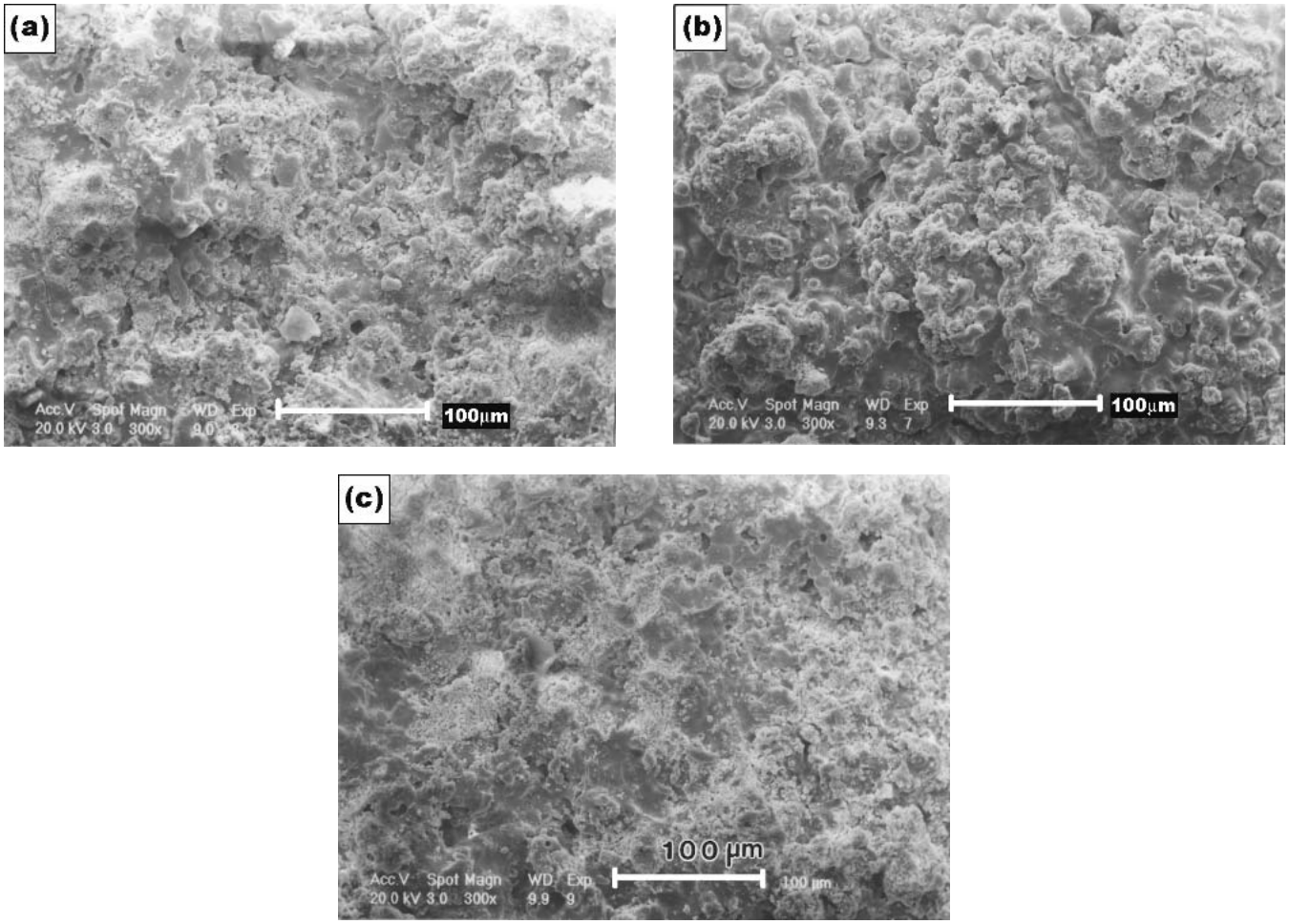

Fig. 4 SEM surface morphologies of as-sprayed HA top coats of **(a)** C-HA/ZrO_2, **(b)** N-HA/ZrO_2, and **(c)** H-HA/ZrO_2 specimens

3.2 Bonding Strength and Fractography

The bonding strength data measured by the adhesion test according to ASTM C633-79 are listed in Table 4. Figure 6 shows the variation of bonding strength measurements of HA/ZrO_2 and HA coatings with the substrate temperatures. This figure reveals that in general the bonding strengths of HA and HA/ZrO_2 coatings are decreased with increasing substrate temperature. How-

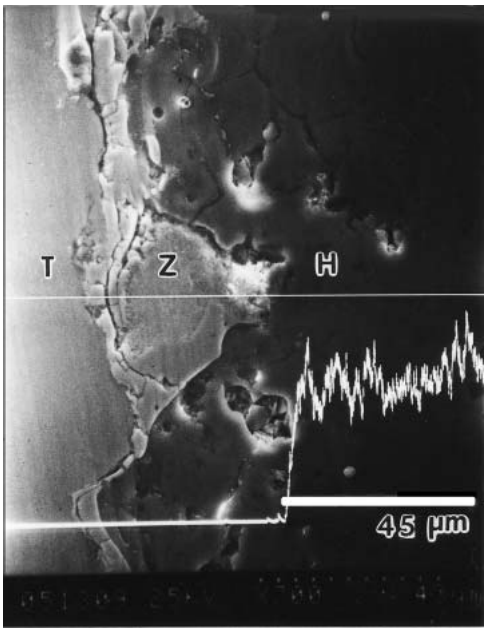

Fig. 5 SEM cross-sectional microstructure of a typical plasma-sprayed HA/ZrO_2 coating with EDS line scan of Ca element distribution. T, Z, and H denote Ti substrate, ZrO_2 and HA, respectively.

Table 4 Results of Bonding Strength Measurements and Area Fraction of Adhesive Failure

Coatings	Bonding Strength, MPa	% ad. Failure
C-HA	32.1 ± 3.5	23.6 ± 5.1
N-HA	28.6 ± 3.2	26.8 ± 5.2
H-HA	23.8 ± 4.1	28.7 ± 5.5
C-HA/ZrO_2	40.8 ± 4.3	14.1 ± 3.7
N-HA/ZrO_2	36.2 ± 3.0	15.8 ± 3.8
H-HA/ZrO_2	43.0 ± 5.6	13.5 ± 3.6

Values are given as mean ± S.D. from 10 tests data. Significance in difference among the data are defined by statistical t-test, $p < 0.005$.

ever, one of the HA/ZrO_2 coating increases drastically at the highest deposition temperature of 200 °C (H-HA/ZrO_2), reversing the trend of decreasing bonding strength with increasing substrate temperature for all of the rest HA/ZrO_2 and HA coatings. In addition, the bonding strengths of C-, N-, and H-HA/ZrO_2 coatings are higher than the respective C-, N-, and H-HA coatings. Statistical *t*-test reveals that the bonding strength obtained in each coating is significantly different from the others ($p <$ 0.005).

The typical optical morphology of the fracture surface of HA/ZrO_2 coating after the ASTM C633-79 test is shown in Fig. 7. The fracture surface indicates that the measured bonding strength is a combination of adhesive (coating to substrate) and cohesive (within the inter- and intra-lamellar structure of coating) strength. Furthermore, the fracture surface of the remained HA/ZrO_2 coating on Ti substrate after adhesion test is subjected to SEM inspection (using both SEI and BEI) and the typical results are shown in Fig. 8. From the comparison of Fig. 8(a) and (b), the locations of ZrO_2, Ti substrate and HA top coat in Fig. 8(a) can be manifested by the corresponding white, gray and

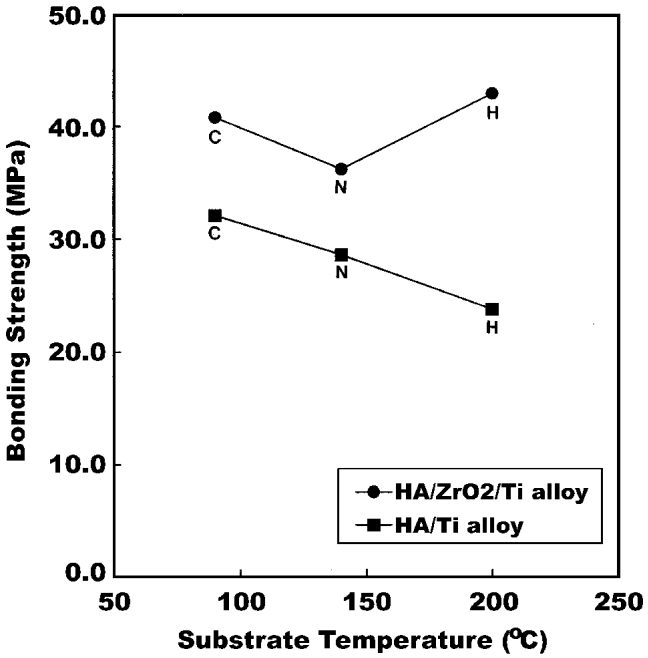

Fig. 6 Variation of bonding strengths of HA/ZrO_2 and HA coatings with the substrate temperatures. C, N and H denote substrate temperatures of 90, 140, and 200 °C, respectively.

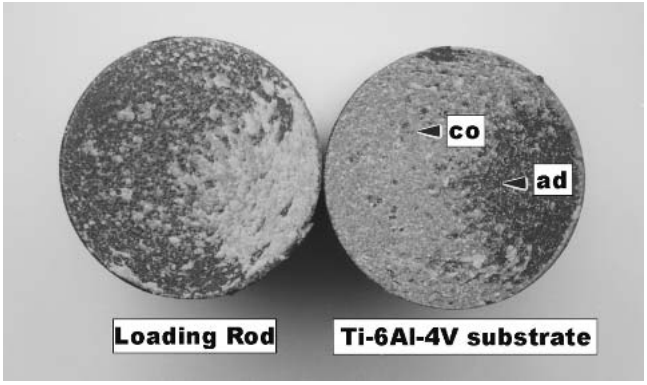

Fig. 7 Optical fractography of a typical HA/ZrO_2 coating on Ti-6Al-4V substrate after the ASTM C633-79 test. In all of the HA/ZrO_2 coatings investigated, the bonding strength measured was a manifestation of cohesive (co) and adhesive (ad) strength.

dark contrasts in Fig. 8(b), respectively. Figure 8(c) shows a typical cohesive failure of the HA/ZrO_2 coating indicating that the crack proceeds within the HA top coat. From the above results, the area percentage of adhesive failure in each coating was further calculated according to the image analysis and reported as the mean ±S.D. from ten specimens (Table 4). The relationship between the bonding strength and the area fraction of adhesive failure for HA/ZrO_2 and HA coatings is reported in Fig. 9.

4. Discussion

4.1 Phase Content

The original ZrO_2 powder stabilized with 8 mol% Y_2O_3 from TOSOH is a cubic phase (JCPD 30-1468). The crystal structures

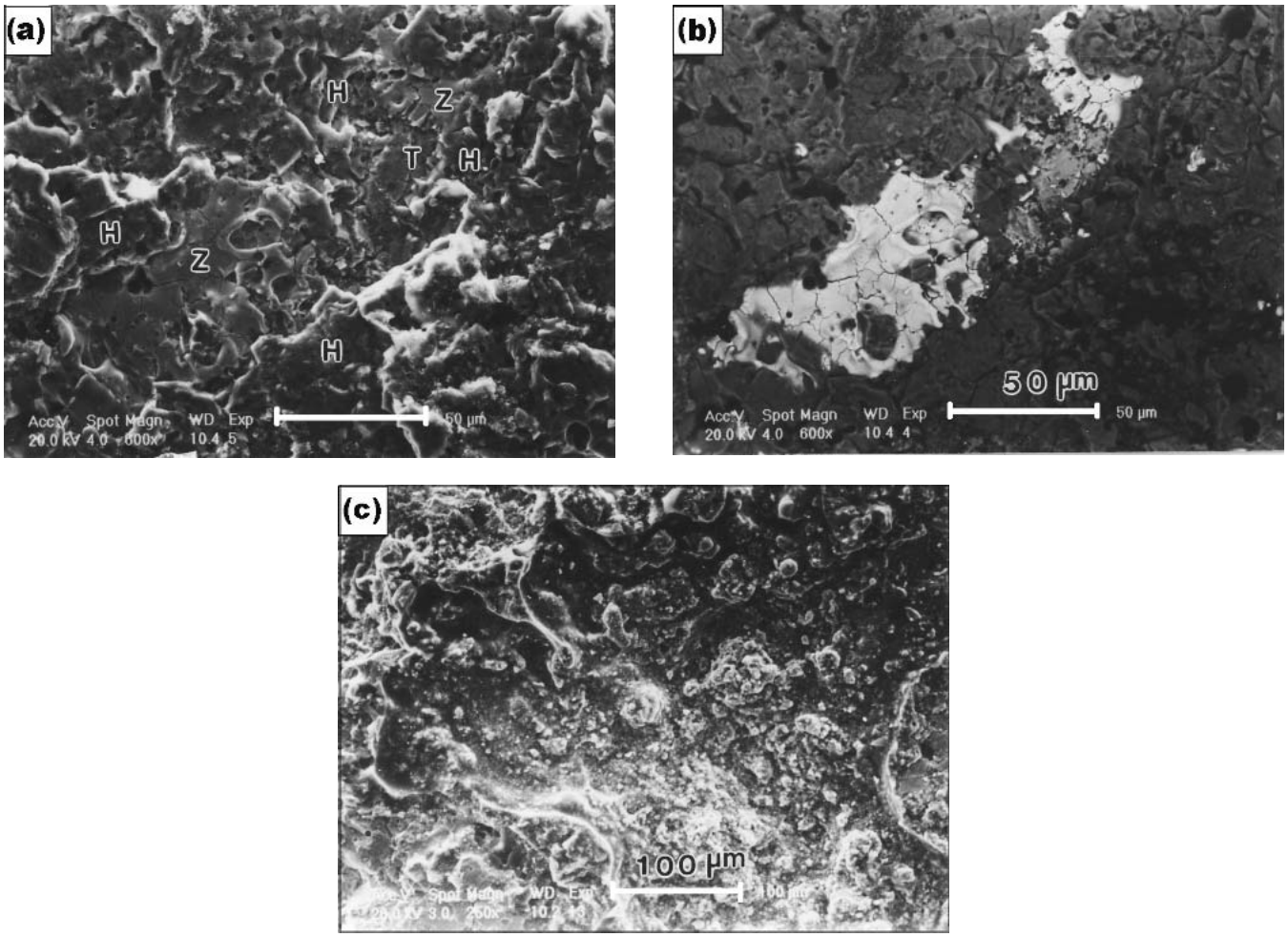

Fig. 8 SEM fractography of HA/ZrO_2 coating remained on Ti-6Al-4V substrate after the ASTM C633-79 test: **(a)** failure occurred at ZrO_2/ Ti-6Al-4V interface and within ZrO_2 bond coat (SEI contrast), **(b)** BEI contrast of **(a)**, and **(c)** failure occurred within HA top coat. T, Z, and H denote Ti alloy substrate, ZrO_2 and HA, respectively.

of the as-sintered ZrO_2 powder suitable for plasma spraying (Fig. 1a) and the as-sprayed ZrO_2 bond coat on the Ti-6Al-4V substrate (Fig. 1b) are also cubic. It is reported that ZrO_2 powder (3~4.5 mol% Y_2O_3 stabilizer), with mixed tetragonal and cubic phases initially, will transform into quenched-in nontransformable tetragonal phase with minor cubic and monoclinic phases during the plasma spraying.[21] Hence, it is believed that the cause of the maintenance of cubic ZrO_2 phase in the current study is the higher content of Y_2O_3 stabilizer. The phase content of the as-sintered HA powder (Fig. 2a) has changed in the HA top coat (Fig. 2b) by the appearance of impurity phases, such as α-TCP, T.P., and CaO. These impurity phases are the products of the decomposition of HA during plasma spraying and the results are consistent with the literature.[22,23]

Moreover, the contents of impurity phases in HA coatings near the HA/ZrO_2 interface (Table 2) reveal that the impurity phases do not change with the variation of substrate temperatures. The contents of impurity phases are, however, significantly lower than those near the top layer of HA coatings by x-ray diffraction analyses. The reason might be that the top layer of HA coatings has experienced higher temperature and longer time for the phase decomposition to take place.

4.2 Coating Structure

The SEM surface of ZrO_2 bond coat [Fig. 3(b)] is evidently rougher than the surface morphology of the grit-blasted Ti substrate (Fig. 3a). The observation seems to be consistent with the measured values of surface roughness listed in Table 3. Lower fracture toughness and bonding strength were reported to correlate with the lower surface roughness of the Ti substrate.[24] Hence, the rougher surface provided by ZrO_2 bond coat is thought to be one of the strengthening mechanisms, which contribute to the performance of HA/ZrO2, coating system. The bonding strengths of C-, N-, and H-HA/ZrO_2 coatings are consistently higher than the respective C-, N-, and H-HA coatings (Table 4 and Fig. 6). In addition, it is noted that the surface roughness of HA coating with a ZrO_2 bond coat is slightly higher than the one without (Table 3). This is obviously caused by the rougher ZrO_2 intermediate layer for the top coating of HA. However, from Table 3 it is seen that the surface roughness of H-series specimens is lower than N- and C-series specimens, while the surface roughness between N- and C-series specimens does not exhibit significant differences (statistical t-test, $p < 0.005$). This observation is also evidenced by the SEM investigation as

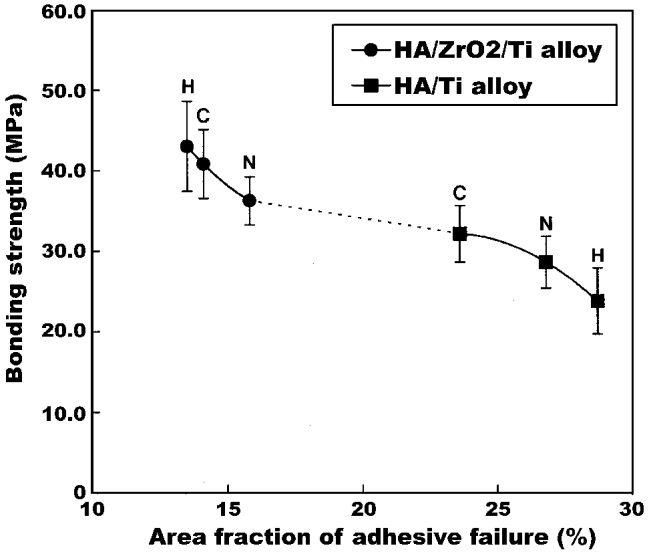

Fig. 9 Variation of bonding strength with the area fraction of adhesive failure for HA/ZrO_2 and HA coatings. C, N, and H denote substrate temperatures of 90, 140, and 200 °C, respectively.

shown in Fig. 4. The surface morphology of H-HA/ZrO_2 shown in Fig. 4(c) displays more smooth features on the surface of the cumulated splats than that of C- and N-HA/ZrO_2 (Fig. 4a and 4b).

Since the degree of melting of the coatings is similar among the HA coatings and HA in HA/ZrO_2 coatings, generally dense structures of HA with similar amounts of porosity are observed from the SEM cross-section of the specimens, with the porosity varying from 5.8-6.9%. The densities of HA in H-HA and H-HA/ZrO_2 coatings are found slightly higher than the C-HA, C-HA/ZrO_2 and N-HA, N-HA/ZrO_2 coatings. The apophyses as shown in Fig. 5 have contributed to the increase of surface roughness and surface area provided for the subsequent deposition of HA. In addition, since the apophyses structure of ZrO_2 bond coat should serve as an anchorage for HA top coat, the toughness of ZrO_2 is likely to play a role in the bonding strength performance as discussed later.

4.3 Bonding Strength and Fractography

The bonding strengths of HA/ZrO_2 coatings and HA coatings generally decrease with increasing substrate temperatures, except for the H-HA/ZrO_2 specimen (Fig. 6). It has been speculated that the residual stress might play a role in the bonding strength of the plasma-sprayed coatings. Recently, the effect of residual stress on the bonding strength of plasma-sprayed HA coating on Ti substrate has been reported.[20] It was found that the state of the residual stress in HA coating was compressive. The findings are consistent with the arguments that compressive stress produces a tensile stress normal to the plane of the coating, which acts on any pre-existing flaws and defects to promote delamination of the coating.[25,26] This effect should lower the bonding strength of coating. In other literature, either compressive and tensile residual stresses were reported[27,28]; however, it was generally accepted that residual stress should be detrimental to the bonding strength.

Residual stress in plasma-sprayed coatings is influenced by the processing variables including substrate temperatures.[18,19,29] The main cause of the generation of residual stress is the thermal expansion mismatch between the coating and the substrate during secondary cooling of substrate to ambient temperature after plasma spraying. As the substrate temperature is increased the amount of contraction mismatch on cooling increases producing greater residual stress. But other factors such as the plasma temperature and the temperature distribution in the coating may greatly complicate the mechanisms of the residual stresses. This complicated phenomenon should be further studied. It has been generally found that the residual stress increases with increasing substrate temperature and that a bond coat on the metallic substrate should not vary the residual stress state of the top coat significantly.[18,19]

The relation between the substrate temperature and the bonding strength of HA and HA/ZrO_2 coatings has not been documented in the literature. Producing an HA coating with higher bonding strength via the variation of substrate temperature and the introduction of a ZrO_2 bond coat was the purpose of the present investigation. The results of Fig. 6 show that the bonding strength increases with decreasing substrate temperature except the H-HA/ZrO_2 specimen. This indicates that a manipulation of substrate temperature during plasma spraying might furnish a method conducive to the bonding strength improvement. The rationale of the relation in Fig. 6 is that an increase of substrate temperature increases the residual stress,[18,19] which in turn decreases the bonding strength.[20]

The above arguments cannot explain the result wherein the bonding strength increases with increasing substrate temperature from 140-200 °C for HA/ZrO_2 coating (Fig. 6). The slightly better molten state of HA in H-HA/ZrO_2 coating (Table 3 and Fig. 4c) should not be a cause, since the phenomenon is similarly observed in H-HA coating (Table 3). In latter coating, the bonding strength decreases with increasing substrate temperature from 140-200 °C (Fig. 6). Hence, it is believed that the slightly denser structure obtained in H-series specimen is not enough to counterweigh the negative effect from the residual stress.

It has been discussed that the apophyses increase the surface roughness and surface area for bonding between HA and ZrO_2 bond coat (Fig. 5). The apophyses structure of ZrO_2 bond coat should serve as an anchorage of HA top coat, where the toughness of ZrO_2 is likely to play a role. The characteristic adhesive failure of HA/ZrO_2 coating shown in Fig. 8(a) and (b) demonstrates that the toughness of ZrO_2 might play a role in the bonding strength performance on the basis that the cracks are found to propagate through the presumed tougher ZrO_2 bond coat. Consequently, the strengthening of HA/ZrO_2 interface by several mechanical mechanisms can explain the generally higher bonding strength of HA/ZrO_2 coatings as compared with the HA coatings as suggested in Fig. 6 (e.g., C-HA/ZrO_2 versus C-HA; N-HA/ZrO_2 versus N-HA). The unusual increase of bonding strength of H-HA/ZrO_2 specimen, compared with H-HA specimen, must be due to other causes.

From our previous study, an elemental interdiffusion between HA top coat and ZrO_2 bond coat was evidenced by TEM in H-HA/ZrO_2 coating.[16] Similar unreported investigations were conducted for N and C specimens, but the calcium diffusion at the HA/ZrO_2 interface was concluded insignificant. The

results indicate that an effective chemical diffusion between HA top coat and ZrO_2 bond coat occurs at the substrate temperatures beyond 140 °C during deposition of HA top coat. Hence it is believed that a stronger diffusion bonding is formed at HA and ZrO_2 interface in H-HA/ZrO_2 as compared with C- and N-HA/ZrO_2 coatings. The relationship in Fig. 9 suggests that the bonding strength of the HA/ZrO_2 and HA coatings is reasonably well correlated with the area fraction of adhesive failure. In drawing Fig. 9 an assumption was made that the processes for producing HA/ZrO_2 and HA coatings were similar; hence a dotted line can be linked between the data of the two-series coatings in Fig. 9. This figure together with Fig. 6 suggest that the bonding strength of HA coating can be improved via increasing the bonding at HA and Ti substrate or decreasing the area fraction of adhesive failure. The goal can be achieved by imposing a ZrO_2 bond coat between HA and Ti substrate and by decreasing the substrate temperature in general. In an unusual case the bonding strength of HA/ZrO_2 coating can be greatly enhanced by purposely preheating the substrate temperature prior to plasma spraying, which increases the bonding between HA top coat and ZrO_2 bond coat chemically through the interdiffusion between them.

5. Summary

Hydroxyapatite coatings were plasma sprayed on the Ti substrate with and without an intermediate ZrO_2 layer; meanwhile the temperatures of Ti substrate and ZrO_2/Ti substrate were varied at 90, 140, and 200 °C. The purpose of the current study was to investigate the individual and combined effects of those processing variables on the bonding strength and failure behavior of the system.

It is found that the bonding strengths of HA/ZrO_2 and HA coatings generally decrease with increasing substrate temperature, except for the H-HA/ZrO_2 specimen deposited at 200 °C. The rationale of the effect of substrate temperature is attributed to the residual stress reported in the literature. Introducing ZrO_2 bond coat is found to significantly promote the bonding strength of HA top coat. The possible strengthening mechanism is the rougher surface provided by ZrO_2 bond coat, which promotes a mechanical interlocking between HA, and ZrO_2. Additionally the higher toughness of ZrO_2 could also play a role in the strengthening effect.

The slightly denser HA in H-HA/ZrO_2 coating cannot explain the high bonding strength of the coating, nor the mechanical strengthening effect of ZrO_2 intermediate layer should apply. From our previous study, an elemental interdiffusion between HA top coat and ZrO_2 bond coat was evidenced by TEM in H-HA/ZrO_2 coating. It is believed that a stronger diffusion bonding is formed at HA/ZrO_2 interface in H-HA/ZrO_2 as compared with C- and N-HA/ZrO_2 coatings.

The bonding strengths of HA/ZrO_2 and HA coatings are correlated with the area fraction of adhesive failure. In general, either imposing a ZrO_2 bond coat between HA and Ti substrate or decreasing the substrate temperature can improve the bonding of HA with Ti substrate, therefore decreasing the area fraction of adhesive failure. In an unusual case the bonding strength of HA/ZrO_2 coating can be greatly enhanced by purposely preheating the substrate temperature prior to plasma spraying, which increases the bonding between HA and ZrO_2 chemically through the interdiffusion between them.

References

1. L.L. Hench: "Bioceramics: From Concept to Clinic," *J. Am. Ceram. Soc.,* 1991, *74,* pp. 1487-510.
2. R.G.T. Geesink, K. deGroot, and C.P.A.T. Klein: "Bone Bonding to Apatite Coated Implants," *J. Bone Joint Surg.,* 1988, *70B,* pp. 17-22.
3. H. Oonishi, M. Yamamoto, H. Ishimaru, E. Tsuji, S. Kushitani, M. Aono, and Y. Ukon: "The Effect of Hydroxyapatite Coating on Bone-Growth Into Porous Titanium-Alloy Implants," *J. Bone Joint Surg.,* 1989, *71B,* pp. 213-16.
4. D. Poulmaire, M. Ducos, Y. Setti, and M.P. Hypolite: "Development of Dental Implants in Titanium With HA Coatings" in *Proc. 2nd Plasma-Technik-Symp.,* Vol. 3, S. Blum-Sandmeier, H. Eschnauer, P. Huber, and A.R. Nicoll, ed., Plasma-Technik AG, Wohlen, Switzerland, 1991, pp. 191-202.
5. D. Matejka, V. Palka, M. Brezovsky, P. Sebo, I. Infner, and M. Pastorok: "Plasma Coated Composite Intraosseous Implants" in *Proc. 2nd Plasma-Technik-Symp.,* Vol. 3, S. Blum-Sandmeier, H. Eschnauer, P. Huber, A.R. Nicoll, ed., Plasma-Technik AG, Wohlen, Switzerland, 1991, pp. 171-77.
6. C.C. Berndt, G.N. Haddad, A.J.D. Farmer, and K.A. Gross: "Thermal Spraying for Bioceramic Applications," *Mater. Forum*, 1990, *14,* pp. 161-73.
7. F. Brossa, A. Cigada, R. Chiesa, L. Paracchini, and C. Consonni: "Adhesion Properties of Plasma Sprayed Hydroxyapatite Coatings for Orthopaedic Prostheses," *Biomed. Mater. Eng.,* 1993, *3,* pp. 127-36.
8. Y. Yang, Z. Liu, C. Luo, and Y. Chuang: "Measurements of Residual Stress and Bonding Strength of Plasma Sprayed Laminated Coatings," *Surf. Coat. Technol.,* 1997, *89,* pp. 97-100.
9. Ö. Ünaland and D.J. Sordelet: "In-Plane Tensile Strength and Residual Stress in Thick Al_2O_3 Coatings on Aluminum Alloy," *Scripta Mater.*, 2000, *42,* pp. 631-36.
10. K. Hayashi, T. Inadome, T. Mashima, and Y. Sugioka: "Comparison of Bone-Implant Interface Shear Strength of Solid Hydroxyapatite and Hydroxyapatite-Coated Titanium Implants," *J. Biomed. Mater. Res.,* 1993, *27,* pp. 557-63.
11. W.J.A. Dhert, C.P.A. T. Klein, J.G.C. Wolke, E.A. vanderVelde, K. deGroot, and P.M. Rozing: "A Mechanical Investigation of Fluorapatite, Magnesiumwhitlockite, and Hydroxyapatite Plasma-Sprayed Coatings in Goats," *J. Biomed. Mater. Res.,* 1991, *25,* pp. 1183-200.
12. B.C. Wang, T.M. Lee, E. Chang, and C.Y. Yang: "The Shear Strength and the Failure Mode of Plasma Sprayed Hydroxyapatite Coating to Bone: The Effect of Coating Thickness," *J. Biomed. Mater. Res.,* 1993, *27,* pp. 1315-27.
13. H. Kurzweg, R.B. Heimann, T. Troczynski, and M.L. Wayman: "Development of Plasma-Sprayed Bioceramic Coatings With Bone Coats Based on Titania and Zirconia," *Biomaterials*, 1998, *19,* pp. 1507-11.
14. Y.C. Tsui, C. Doyle, and T.W. Clyne: "Plasma Sprayed Hydroxyapatite Coatings on Titanium Substrates, Part 2: Optimization of Coating Properties," *Biomaterials*, 1998, *19,* pp. 2031-43.
15. D. Lamy, A.C. Pierre, and R.B. Heimann: "Hydroxyapatite Coatings With a Bond Coat of Biomedical Implants by Plasma Projection," *J. Mater. Res.,* 1996, *11*(3), pp. 680-86.
16. B.Y. Chou and E. Chang: "Interface Investigation of Plasma-Sprayed Hydroxyapatite Coating on Titanium Alloy With ZrO_2 Intermediate Layer as Bond Coat," *Scripta Mater.*, 2001, *45,* pp. 487-93.
17. R. Elsing, O. Knotek, and U. Balting: "The Influence of Physical Properties and Spraying Parameters on the Creation of Residual Stresses During the Spraying Process," *Surf. Coat. Technol.,* 1990, *41,* pp. 147-56.
18. S. Takeuchi, M. Ito, and K. Takeda: "Modelling of Residual Stress in Plasma-Sprayed Coatings: Effect of Substrate Temperature," *Surf. Coat. Technol.,* 1990, *43/44,* pp. 426-35.
19. P. Scardi, M. Leoni, and L. Bertamini: "Residual Stress in Plasma Sprayed Partially Stabilized Zirconia TBCs: Influence of the Deposition Temperature," *Thin Solid Films*, 1996, *278,* pp. 96-103.
20. Y.C. Yang and E. Chang: "Influence of Residual Stress on Bonding Strength and Fracture of Plasma-Sprayed Hydroxyapatite Coatings on Ti-6Al-4V Substrate," *Biomaterials*, 2001, *22,* pp. 1827-36.
21. R.A. Miller, R.G. Garlick, and J.L. Smialek: "Phase Distribution in Plasma Sprayed Zirconia-Yittria System," *Am. Ceram. Soc. Bull.,* 1983, *62*(12), pp. 1355-59.
22. G. deWith, H.J.A. Vandijk, N. Hattu, and K. Prijs: "Preparation, Micro-

structure and Mechanical Properties of Dense Polycrystalline Hydroxyapatite," *J. Mater. Sci.,* 1981, *16,* pp. 1592-98.
23. M.B. Thomas, R.H. Doremus, M. Jarcho, and R.L. Salsbury: "Dense Hydroxyapatite: Fatigue and Fracture Strength After Various Treatments, From Diametral Tests," *J. Mater. Sci.,* 1980, *15,* pp. 891-94.
24. M.J. Filiaggi, N.A. Coombs, and R.M. Pilliar: "Characterization of the Interface in the Plasma-Sprayed HA Coating/Ti-6Al-4V Implant System," *J. Biomed. Mater. Res.,* 1991, *25,* pp. 1211-29.
25. A.G. Evans, G.B. Crumley, and R.E. Demaray: "On the Mechanical Behavior of Brittle Coatings and Layers," *Oxidat. Met.,* 1983, *20,* pp. 196-216.
26. R. Mevrel: "Cyclic Oxidation of High-Temperature Alloys," *Mater. Sci. Technol.,* 1987, *3,* pp. 531-35.
27. V. Sergo, O. Sbaizero, and D.R. Clarke: "Mechanical and Chemical Consequences of the Residual Stresses in Plasma Sprayed Hydroxyapatite Coatings," *Biomaterials*, 1997, *18*(6), pp. 477-82.
28. Y. Han, J. Nan, and K. Xu: "Residual Stresses in Plasma-Sprayed Hydroxyapatite Coatings," *J. Mater. Sci. Lett*., 1999, *18,* pp. 1087-89.
29. J.W. Watson and S.R. Levine: "Deposition Stress Effects on the Life of Thermal Barrier Coatings on Burner Rigs," *Thin Solid Films*, 1984, *119,* pp. 185-93.